



OPTIMIZATION OF PHOTOCATALYTIC ACTIVITY OF Mg/ZnO NANOPARTICLES IN THE REMOVAL OF A MODEL CONTAMINANT USING RESPONSE SURFACE METHODOLOGY

Nahide Zarei, Mohammad Ali Behnajady*

Department of Chemistry, Tabriz Branch, Islamic Azad University, Tabriz, Iran

Abstract

In this study, Mg-doped ZnO nanoparticles with 2% Mg content were synthesized by sol-gel method. The structure and morphology of the nanoparticles were characterized by TEM, BET and UV-Vis absorbance techniques. From TEM image, it was found out that the nanoparticles had uniform size and uniform distribution. BET analysis revealed that in comparison with pure ZnO, Mg 2%/ZnO nanoparticles had a higher specific surface area. Based on UV-Vis absorbance analysis, Mg 2%/ZnO nanoparticles shifted to a lower wavelength (blue-shift), showing a high photocatalytic activity under UV light irradiation. The central composite design under the response surface methodology (RSM) was used for optimization of the photocatalytic removal of Rhodamine B (RhB) with Mg 2%/ZnO nanoparticles. The results showed that there was a good agreement between the predicted data from RSM and the experimental data with a correlation coefficient of 0.9354. The determined optimum values for removal of RhB were as follows: Mg 2%/ZnO nanoparticles dosage of 500 mg L⁻¹, initial RhB concentration of 6 mg L⁻¹, the irradiation time of 6 min, and pH = 8. In order to get more information about photocatalytic activity of the prepared Mg 2%/ZnO nanoparticles, a comparison was made between the photocatalytic activity in this study and that reported by other researchers. The results revealed the synthesized Mg 2%/ZnO nanoparticles had considerable photocatalytic activity.

Keywords: Mg/ZnO, photocatalytic activity, Rhodamine B, response surface methodology

Received: November, 2014; Revised final: May, 2015; Accepted: June, 2015; Published in final edited form: February, 2019

1. Introduction

The production and use of synthetic chemical products have experienced an important increase during the last century (Cotto-Maldonado et al., 2013). Generally, dyes are used in industries like textiles, plastics, leather, food, cosmetics and pharmaceuticals (Narayana Saibaba et al., 2011). Most dyes are highly toxic, carcinogenic, and resistant against degradation (Tian et al., 2011). The commonly applied water treatment methods for the removal of dyes including chemical, physical and biological processes are inadequate because these contaminants have high molecular weight and biochemical stability (Cotto-Maldonado et al., 2013). In recent years, advanced

oxidation processes (AOPs) have attracted considerable attention as a replacement for the other traditional wastewater treatment methods (Behnajady et al., 2008a, 2011a; Zuorro et al., 2013). Among the AOPs, the heterogeneous photocatalysis process employing semiconductor catalysts (such as ZnO, TiO₂, Fe₂O₃, CdS, and ZnS) has demonstrated its efficiency in degrading the refractory compounds which change the pollutants into carbon dioxide, water and inorganic acid (Behnajady et al., 2009, 2011b; Behnajady and Eskandarloo, 2013; Chong et al., 2010; Eskandarloo et al., 2015; Jonidi Jafari et al., 2016; Khalik et al., 2018; Montazerozohori and Hoseinipour, 2017; Moussavi et al., 2015). The major drawback of heterogeneous photocatalytic process is

*Author to whom all correspondence should be addressed: e-mail: behnajady@gmail.com, behnajady@iaut.ac.ir; Phone: +98-41-33396025; Fax: +98-41-33333458

the fast recombination rate of the electron-hole pairs (Ahmed et al., 2011a). Doping of semiconductors with selected elements is an effective route in order to reduce the electron-hole recombination rate by trapping the electrons (Behnajady et al., 2008b; Guerra et al., 2012). Also, doping of semiconductors with metals can increase the specific surface area, decrease the particle size and consequently enhance the photocatalytic activity (Ahmed et al., 2011b; Lutic et al., 2017). The doping of ZnO with a metal could change its conductivity, room temperature ferromagnetism, and sensing properties (Karthikeyan and Pandiyarajan, 2010). Also, doping with Mg may adjust the value of the band gap and increase the UV luminescence intensity (Viswanatha et al., 2012). Mg doped ZnO has been prepared using various techniques such as sonochemical method (Xianyong et al., 2011), precipitation (Viswanatha et al., 2012), sol-gel (Huang et al., 2012), mechanical milling (Suwanboon and Amornpitoksuk, 2012) and chemical vapor deposition (Lin et al., 2004). Among these methods, the sol-gel process is an attractive method because of its simplicity, reproducibility and cheap price (Huang et al., 2012; Umar et al., 2013).

Response surface methodology (RSM) is a collection of experimental design techniques that uses statistical and mathematical methods for designing experiments (Eskandarloo et al., 2014; Khataee, 2009; Trinh and Kang, 2010). RSM consists of an adequate functional relationship between a response of interest and a number of associated control variables (Khuri and Mukhopadhyay, 2010).

The purpose of RSM method is to find optimum response and realize how the response changes in a given direction by modulating the design variables. Two common designs used in RSM are central composite design (CCD) and Box-Behnken design, but the CCD is the most commonly selected method in RSM technique (Bradley, 2007; Sudamalla et al., 2012). Optimization by RSM for several water treatment processes such as Fenton-like (Pajootan et al., 2014; Xu et al., 2013), electrocoagulation (Olmez, 2009; Pi et al., 2014; Zhao et al., 2014), photocatalytic degradation (Khataee, 2010; Khataee et al., 2011; Shaykhi and Zinatizadeh, 2014; Tzikalos et al., 2013; Vaez et al., 2012), electro-oxidation (Saravanathan et al., 2007) and adsorption (Fakhri, 2015; Fakhri and Behrouz, 2015; Zolgharnein et al., 2010) have been reported.

Results of our previous work (Zarei & Behnajady, 2016) indicated that maximum photocatalytic activity was achieved for Mg/ZnO nanoparticles with 2% Mg content. Therefore in this work RSM has been used for optimization of Mg 2%/ZnO nanoparticles photocatalytic activity. To the best of our knowledge, the RSM optimization of photocatalytic activity of Mg/ZnO nanoparticles has not been reported. In the present study, the photocatalytic activity of Mg/ZnO nanoparticles in the removal of RhB as a model contaminant has been optimized by the CCD method.

2. Material and methods

2.1. Materials

Zinc acetate, ethanol, RhB and oxalic acid were obtained from Merck and magnesium nitrate was purchased from Scharlu. RhB is a dye that belongs to a class of compounds called xanthenes with a molecular weight of 479.02 g mol⁻¹ and a formula C₂₈H₃₁N₂O₃Cl. The molecular structure of RhB is given in Fig. 1.

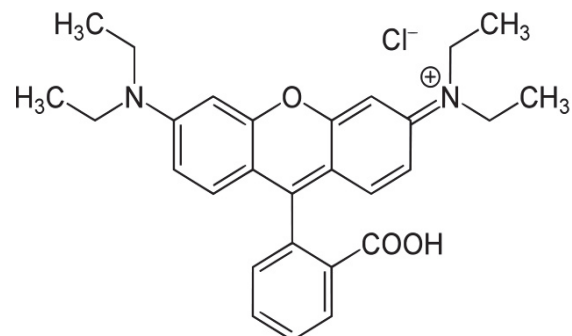


Fig. 1. Molecular structure of RhB

2.2. Synthesis of Mg 2%/ZnO nanoparticles

To prepare Mg 2%/ZnO nanoparticles, first, zinc acetate di-hydrate was dissolved in ethanol at 60 °C and stirred for 30 min; then the oxalic acid which had been dissolved in ethanol at 60 °C was added drop-wise to the zinc acetate solution. 2.0 wt% of magnesium nitrate dissolved in ethanol were added drop-wise to the zinc acetate-oxalic acid solution being stirred. The suspension was stirred for 2 h and dried at 80 °C for 12 h. Finally, the dried powder was calcined at 400 °C for 2 h (Georgekutty et al., 2008).

2.3. Characterization of Mg 2%/ZnO nanoparticles

The morphology was studied by Transmission Electron Microscopy using Philips-CM10. The specific surface area of the synthesized samples was determined by Brunauer-Emmett-Teller (Belsorp mini II). UV-Vis absorbance measurements were carried out by TEC-2048-Avaspec as spectrometer.

2.4. Photoreactor and experiments procedure

Photocatalytic removal studies were conducted at ambient temperature using tubular batch quartz reactor of 100 mL, which was positioned parallel to the light source (Fig. 2). The UV-C lamp (15 W, $\lambda_{\text{max}} = 254$ nm, Philips) was used as the irradiation source. Fig. 3 shows the distribution of UV-C lamp light intensity versus light wavelength. In each experiment, a desired amount of catalyst (200 - 600 mg L⁻¹) was dispersed in 50 mL of distilled water for 15 min by sonication (Elma T460/H, 35 kHz, and 170 W). The suspension was added to a desired concentration of

RhB ($4 - 12 \text{ mg L}^{-1}$). After adjusting the pH of the solution to the desired level (5 - 9), and prior to irradiation, the solution was stirred in the dark for 15 min in the presence of oxygen to reach the adsorption-desorption equilibrium.

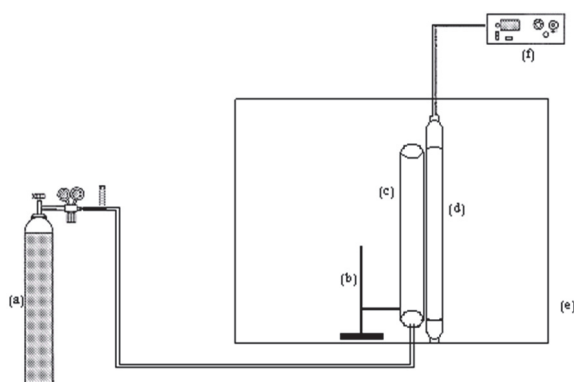


Fig. 2. Schematic diagram of tubular batch quartz photoreactor: (a) O₂ cylinder, (b) clamp, (c) quartz tubular reactor, (d) UV-C lamp, (e) shield and (f) power supply

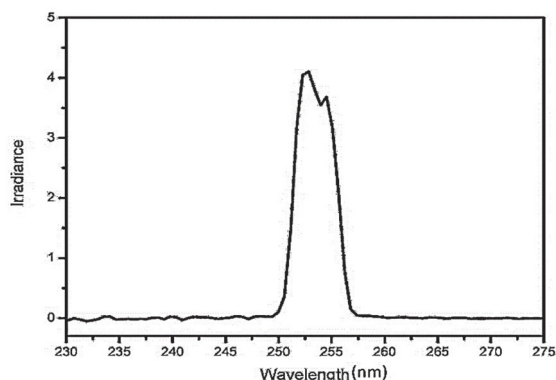


Fig. 3. The distribution of UV-C lamp light intensity versus light wavelength

Then, the suspension was irradiated with UV-C lamp. Samples were collected at specific time intervals and then centrifuged at 1000 rpm (Hettich EBA 8S) for 15 min and filtered to eliminate the catalyst particle completely. Finally, the concentration of RhB was measured using a UV-visible spectrophotometer at $\lambda_{\max} = 554 \text{ nm}$ (Ultrospec 2000, Biotech Pharmacia, England).

2.5. Experimental design

In this study, the CCD was used to optimize the reaction conditions. Mg 2%/ZnO dosage (mg L⁻¹), initial RhB concentration (mg L⁻¹), irradiation time (min) and pH were selected as the main factors, denoted by x_1 , x_2 , x_3 and x_4 , respectively. These parameters are main factors which influences removal rate of the RhB in this process. The factor levels are coded as -1 (low) and +1 (high). The removal efficiency of RhB was chosen as the response parameter. The experimental data were analyzed using the Design-Expert (version 7) software. The design comprised 30 experiments including 16 experiments for full factorial (2^4) and 6 replications at the center point and 8 axial points. The experimental range and levels of independent variables for RhB removal are given in Table 1. The experimental range of variables was selected on the base of preliminary experiments and also other similar works (Xu et al., 2013).

3. Results and discussion

3.1. Characterization of Mg/ZnO nanoparticles

TEM image of Mg 2%/ZnO nanoparticles is shown in Fig. 4. As seen in the figure, the synthesized nanoparticles are of uniform size and uniform distribution and have agglomerated to larger particles.

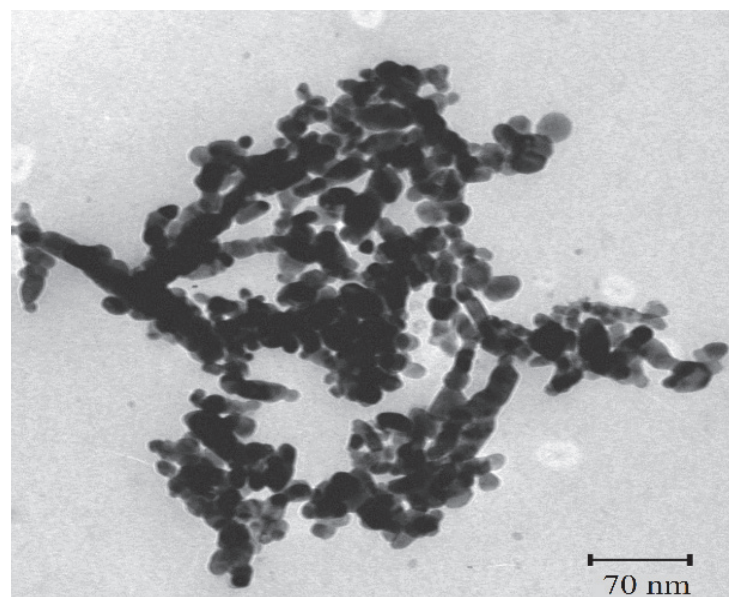


Fig. 4. TEM micrograph of Mg 2%/ZnO nanoparticles

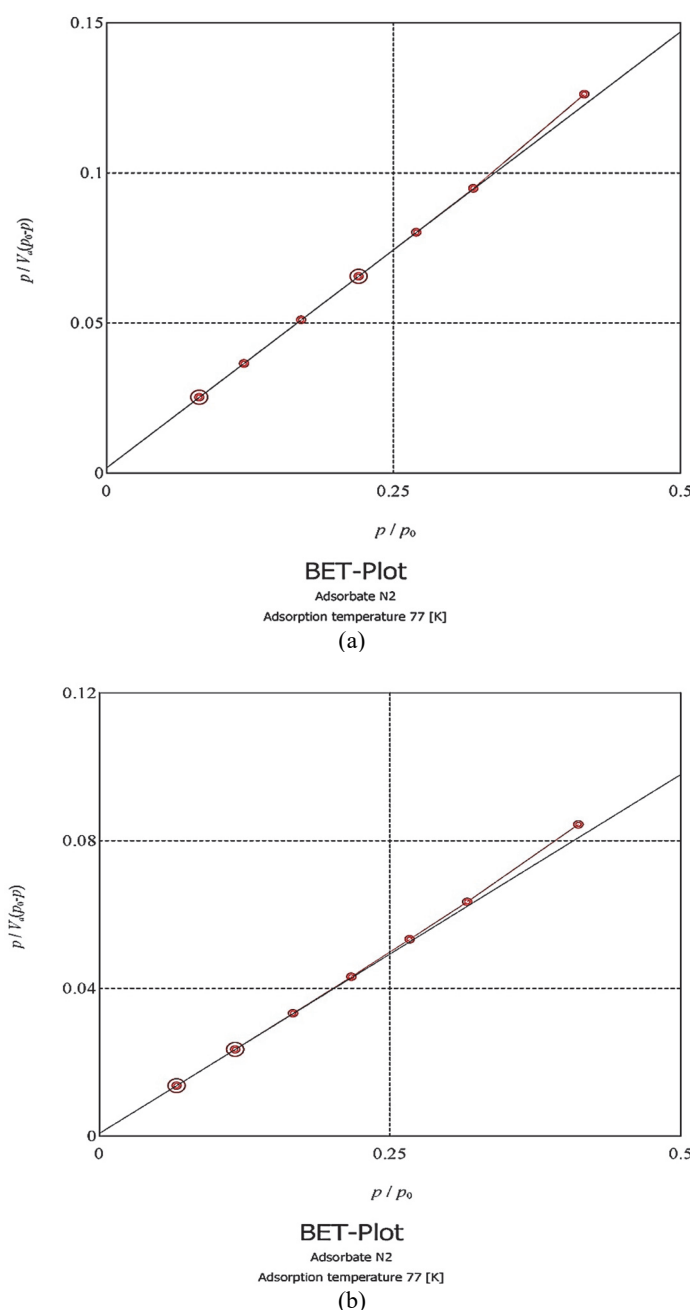
Table 1. Experimental ranges and levels of the variables

Factor	Variable	Coded (Levels)				
		-2	-I	0	+I	+2
X ₁	Mg 2%/ZnO (mg L ⁻¹)	200	300	400	500	600
X ₂	RhB (mg L ⁻¹)	4	6	8	10	12
X ₃	Irradiation time (min)	1.5	3	4.5	6	7.5
X ₄	pH	5	6	7	8	9

The specific surface area was determined using the Brunauer-Emmet-Teller (BET) method (Fig. 5). The specific surface area for ZnO and Mg 2%/ZnO nanoparticles were 14.9 and 22.5 m²g⁻¹, respectively (Zarei & Behnajady, 2016). Fig. 6 shows the absorbance spectra of pure ZnO and Mg 2%/ZnO nanoparticles. As seen, compared to pure ZnO, the Mg 2%/ZnO nanoparticles shifted to a lower wavelength

(blue-shift) so that the doped nanoparticles would not be suitable for visible light.

In other words, under UV light irradiation, Mg 2%/ZnO nanoparticles could have high photocatalytic activity and are not suitable for visible light. Therefore, in this study, photocatalytic activity of Mg 2%/ZnO nanoparticles was investigated under UV light irradiation.

**Fig. 5.** BET diagrams for (a) ZnO and (b) Mg 2%/ZnO nanoparticles

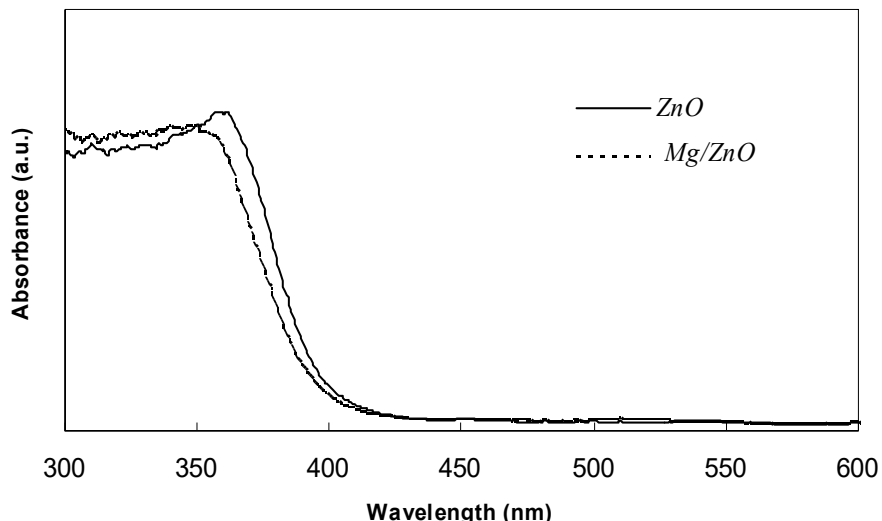


Fig. 6. The absorbance spectra of ZnO and Mg 2%/ZnO nanoparticles

3.2. CCD model and statistical analysis

In the present study, CCD was employed to determine the relation between removal efficiency and operating variables such as photocatalyst dosage, initial RhB concentration, irradiation time and pH within the selected experimental ranges.

According to Table 2, the *F*-value is calculated for each sort of model, and the topmost order model with significant terms is normally selected (Sohrabi et al., 2016). So, the mathematical relationship of the response (*Y*) is explained by Eq. (1):

$$Y = b_0 + b_1x_1 + b_2x_2 + b_3x_3 + b_4x_4 + b_{12}x_1x_2 + b_{13}x_1x_3 + b_{14}x_1x_4 + b_{23}x_2x_3 + b_{24}x_2x_4 + b_{34}x_3x_4 + b_{11}x_1^2 + b_{22}x_2^2 + b_{33}x_3^2 + b_{44}x_4^2 \quad (1)$$

where *Y* is the response variable of removal efficiency, *b*₀ is the constant, *b_i* (*i*=1, 2, 3, and 4), *b_{ij}* and *b_{ii}* (*i*=1, 2, 3, and 4; *j*=1, 2, 3, and 4) are the regression coefficients for linear effects, interaction effects, and quadratic effects, respectively. The obtained second-order polynomial model could be described as follows (Eq. 2):

$$Y = 61.96 + 2.66x_1 - 5.70x_2 + 10.04x_3 + 3.06x_4 - 0.83x_1x_2 + 1.26x_1x_3 + 1.99x_1x_4 - 1.10x_2x_3 + 0.68x_2x_4 + 5.59x_3x_4 - 3.40x_1^2 - 4.67x_2^2 + 0.78x_3^2 - 3.29x_4^2 \quad (2)$$

The predicted photocatalytic removal percentages of RhB using the Mg 2%/ZnO nanoparticles by Eq. (2) are presented in Table 3.

Analysis of variance (ANOVA), which was conducted to evaluate the significance and adequacy of the model, provided information about quadratic and interaction effects along with the normal linearized effects of the parameters (Esfahani et al., 2014; Narayana Saibaba et al., 2011; Olmez, 2009). ANOVA results for the model and variables are presented in Table 4. As evident from this table, the R² of the model is 0.9354, implying that 93.54% of the variations for the photocatalytic removal of RhB are

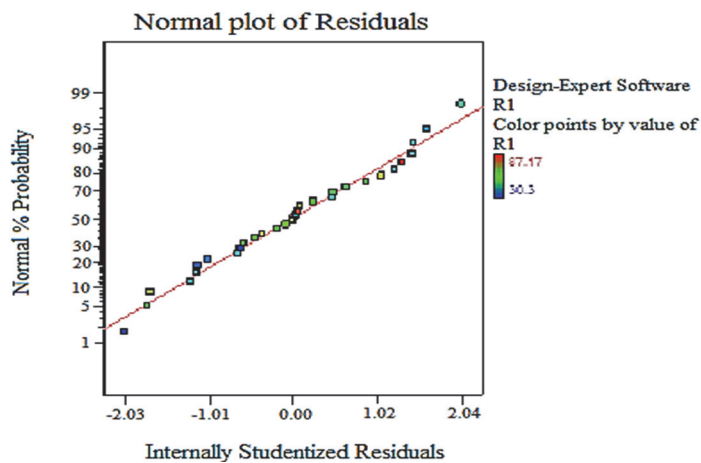
accounted for by the independent variables and just 6.46% of variation cannot be explained by the model. The *F*-value for the model is 15.51, confirming that the model is significant. Values of "Prob > F" less than 0.0500 indicate that the model terms are significant (in this case, A, B, C, D, CD, A², B², D² are significant model terms), while values greater than 0.1000 indicate that the model terms are not significant.

3.3. Response Surface Analysis

The measurement of the residuals is a method to evaluate the adequacy of the model. Normal probability plot is important for judging the normality of the residuals (Khataee, 2009). As seen in Fig. 7, the points are near the diagonal line, indicating low discrepancies between them and adequate for explaining the process under study. Also, the residual plots almost form a straight line, implying that the distribution is normal.

3.3.1. Effects of operational variables

The contour and 3D diagrams are the best approach to learn about the effect of each variable (Esfahani et al., 2014). In Fig. 8, the response surface and contour plots were developed as a function of photocatalyst dosage and initial RhB concentration. As implied from Fig. 8, the removal efficiency of RhB increases with increasing photocatalyst dosage whereas it decreases with increasing the initial RhB concentration. The results revealed that the maximum removal efficiency was achieved at the range of 4 - 8 mg L⁻¹ initial RhB concentration and 400 - 500 mg L⁻¹ of photocatalyst dosage. One way to account for this is that with the increase of the photocatalyst dosage to the proper amount, active sites on the catalyst surface increase and more number of RhB molecules can be adsorbed on the surface of Mg/ZnO photocatalyst. Another explanation is that increasing the catalyst dosage and active sites leads to the formation of more hydroxyl radicals, causing the photocatalytic activity to increase (Nishio et al., 2006).

**Fig. 7.** Normal plot of residual for removal of RhB**Table 2.** Statistical parameters for sequential models

Source	Sum of Squares	df	Mean Square	F Value	P-value Prob>F	
Mean vs Total	85852.52	1	85852.52			
Linear vs Mean	3595.47	4	898.87	10.87	<0.0001	
2FI vs Linear	626.05	6	104.34	1.38	0.2743	
Quadratic vs 2FI	1074.89	4	268.72	11.02	0.0002	suggested
Cubic vs quadratic	121.47	8	15.18	0.44	0.8668	
Residual	244.31	7	34.90			
Total	91514.71	30	3050.49			

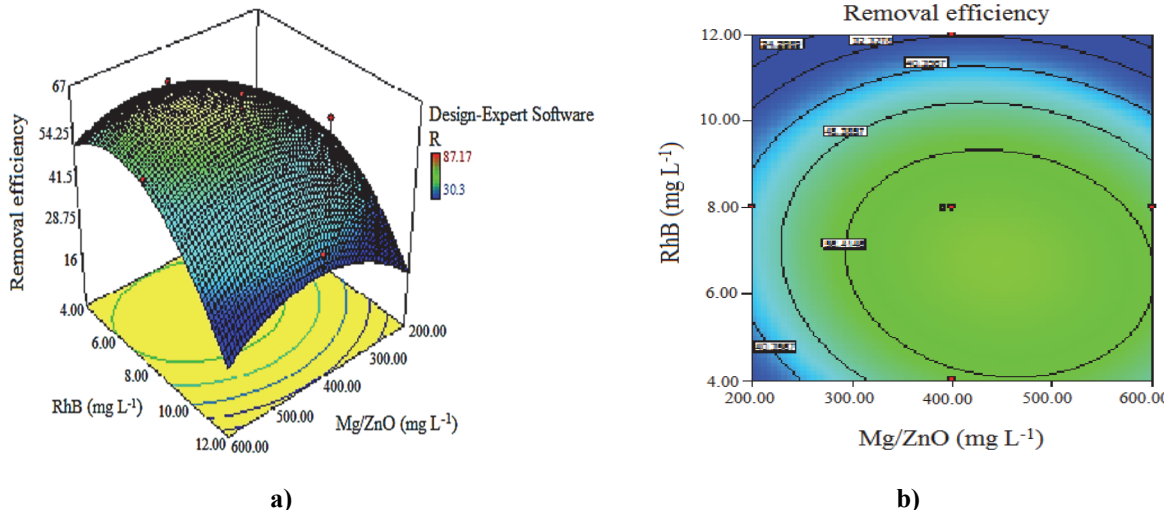
Table 3. The 4-factor CCD matrix and the value of response function

Run	Mg 2%/ZnO (mg L ⁻¹)	RhB (mg L ⁻¹)	Irradiation time (min)	pH	Removal efficiency (%)	
					Experimental	Predicted
1	400 (0)	8 (0)	4.5 (0)	7 (0)	62.37	61.96
2	400 (0)	4 (-2)	4 (0)	7 (0)	56.23	54.67
3	400 (0)	12 (+2)	4.5 (0)	7 (0)	37.02	31.86
4	400 (0)	8 (0)	4.5 (0)	9 (+2)	57.73	54.92
5	400 (0)	8 (0)	4.5 (0)	7 (0)	61.92	61.96
6	400 (0)	8 (0)	1.5 (-2)	7(0)	51.48	44.99
7	600 (+2)	8 (0)	4.5(0)	7 (0)	55.76	53.69
8	500 (+1)	6 (-1)	6 (+1)	6 (-1)	57.39	63.02
9	300 (-1)	10(+1)	3 (-1)	8 (+1)	30.3	32.31
10	500 (-1)	6 (+1)	3 (-1)	6 (-1)	43.23	46.96
11	200 (-1)	8 (+1)	4.5 (-1)	7 (+1)	36.71	40.01
12	500 (-2)	6 (0)	6 (0)	8 (0)	47.69	43.04
13	500 (+1)	6 (-1)	6 (+1)	8 (+1)	87.17	82.94
14	400 (0)	8 (0)	4.5 (0)	7 (0)	61.57	61.96
15	400 (0)	8 (0)	4.5 (0)	7 (0)	66.79	61.96
16	400 (0)	8 (0)	4.5 (0)	7 (0)	59.85	61.96
17	400 (0)	8 (0)	4.5 (0)	7 (0)	59.24	61.95
18	300 (-1)	10 (+1)	6 (+1)	8 (+1)	58.27	58.85
19	300 (-1)	6 (-1)	3 (-1)	6 (-1)	46.77	48.91
20	300 (-1)	6 (-1)	6 (+1)	8 (+1)	68.26	69.44
21	500 (+1)	10 (+1)	6 (+1)	6 (-1)	51.02	46.41
22	300 (-1)	10 (+1)	6 (+1)	6 (-1)	40.29	44.02
23	500 (+1)	6 (-1)	3 (-1)	6 (-1)	50.90	49.39
24	400 (0)	8 (0)	7.5 (+2)	7 (0)	85.38	85.16
25	300 (-1)	6 (+1)	6 (-1)	6 (-1)	58.29	57.49
26	500 (+1)	10 (+1)	3 (-1)	8 (+1)	37.57	37.44
27	400 (0)	8 (0)	4.5 (0)	5 (-2)	46.61	42.70
28	500 (+1)	10 (+1)	3 (-1)	6 (-1)	30.69	37.16
29	500 (+1)	10 (+1)	6 (+1)	8 (+1)	63.53	69.03
30	300 (-1)	6 (-1)	3 (-1)	8 (+1)	34.83	38.51

Table 4. Analysis of variance

Source	Sum of squares	Degree of freedom	Mean square	F-value	P-value Prob>F	
Model	5296.41	14	378.31	15.51	<0.0001	significant
A	170.24	1	170.24	6.98	0.0185	
B	780.67	1	780.67	32.01	<0.0001	
C	2420.44	1	2420.44	99.26	<0.0001	
D	224.11	1	224.11	9.19	0.0084	
AB	11.06	1	11.06	0.45	0.5110	
AC	25.55	1	25.55	1.05	0.3222	
AD	63.30	1	63.60	2.61	0.1271	
BC	19.23	1	19.23	0.79	0.3886	
BD	7.32	1	7.32	0.30	0.5919	
CD	499.30	1	499.30	20.48	0.0004	
A ²	316.57	1	316.57	12.98	0.0026	
B ²	598.77	1	598.77	24.55	0.0002	
C ²	16.64	1	16.64	0.68	0.4217	
D ²	296.18	1	296.18	12.15	0.0033	
Residual	365.78	15	24.39	-	-	
Lack of Fit	330.28	10	33.03	4.65	0.0518	not significant
Pure Error	35.50	5	7.10	-	-	
Cor Total	5662.19	29		-	-	

$$R^2 = 0.9354$$

**Fig. 8.** (a) Response surface and (b) contour plots of RhB removal efficiency (%) as a function of Mg/ZnO dosage and initial RhB concentration

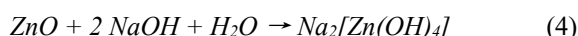
Similar results have been reported by Behnajady et al. (2008) about photocatalytic degradation of Acid Red 88 using Ag/TiO₂ nanoparticles. Cun et al. (2002) also revealed that the formation of 'OH species decreased in presence of excess amount of photocatalyst, causing a decline in the removal efficiency. In high amounts of photocatalyst, it is difficult to maintain the homogeneity of the system because the photocatalyst particles tend to agglomerate, thus reducing the number of active sites on the photocatalyst surface and consequently photocatalytic activity (Ahmed et al., 2011b). The increase of the initial concentration of RhB decreases the penetration of light into the solution and absorption of photons by photocatalyst, leading to a reduction in the formation of electron-hole pair. Other researchers have come up with similar results regarding the effect of increasing the

initial concentration of contaminant on the formation of electron-hole pairs (Talebian and Nilforoushan, 2010; Wu and Chang, 2006).

The effects of Mg/ZnO dosage and irradiation time on the removal efficiency of RhB are shown in Fig. 9. These figures clearly show that RhB removal efficiency increased with the increase of the irradiation time. The highest removal efficiency was achieved at the range of 6 - 7.5 min and 400 - 500 mg L⁻¹ of Mg/ZnO dosage.

The effect of photocatalyst dosage and pH on the removal efficiency of RhB is illustrated in Fig. 10. As evident from the figure, pH rise has a positive effect on the removal of RhB so that increasing pH to the range of 5 - 8 and Mg/ZnO dosage to the range of 200 - 400 mg L⁻¹ causes removal efficiency to increase. In photocatalytic systems, pH is a factor that affects the process rate. As readily inferred from Fig.

10, the removal efficiency in acidic and alkaline conditions is less than that in neutral conditions. RhB is a cationic compound, and in acidic pH values, the catalyst surface which has positive charges is unable to adsorb RhB, leading to a decline in the removal efficiency. Nevertheless, the main reason for the decrease of the photocatalytic activity in acidic and alkaline conditions can be the instability of the ZnO and its dissolution according to Eqs. (3) and (4) (Greenwood and Earnshaw, 1997):



3.3.2. Determination of optimal conditions for operational variables

In this study, the main goal was to evaluate the optimum values of variables for the photocatalytic removal of RhB using CCD method. The optimum values of each variable for the maximum removal efficiency of RhB are presented in Table 5. As apparent from the table, the corresponding experimental value (87.17 %) of removal efficiency of RhB was in good agreement with the predicted response (83.25 %); thus, it can be deduced that RSM is an effective technique to optimize the operational parameters for removal efficiency of RhB by heterogeneous photocatalytic process.

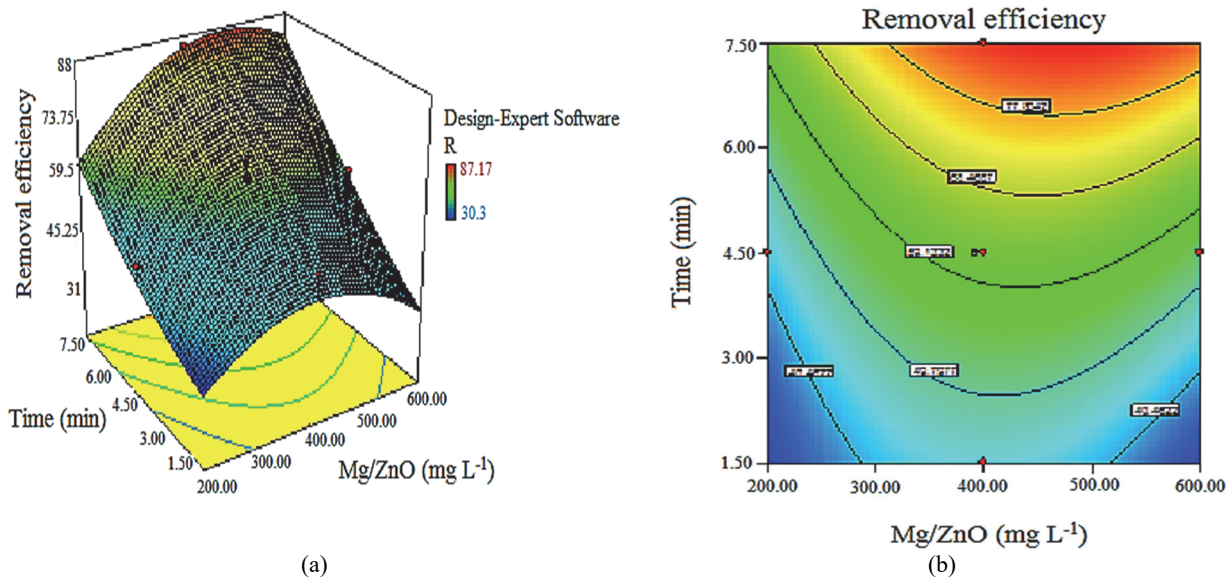


Fig. 9. (a) Response surface and (b) contour plots for photocatalytic removal efficiency of RhB (%) as a function of Mg/ZnO dosage and irradiation time

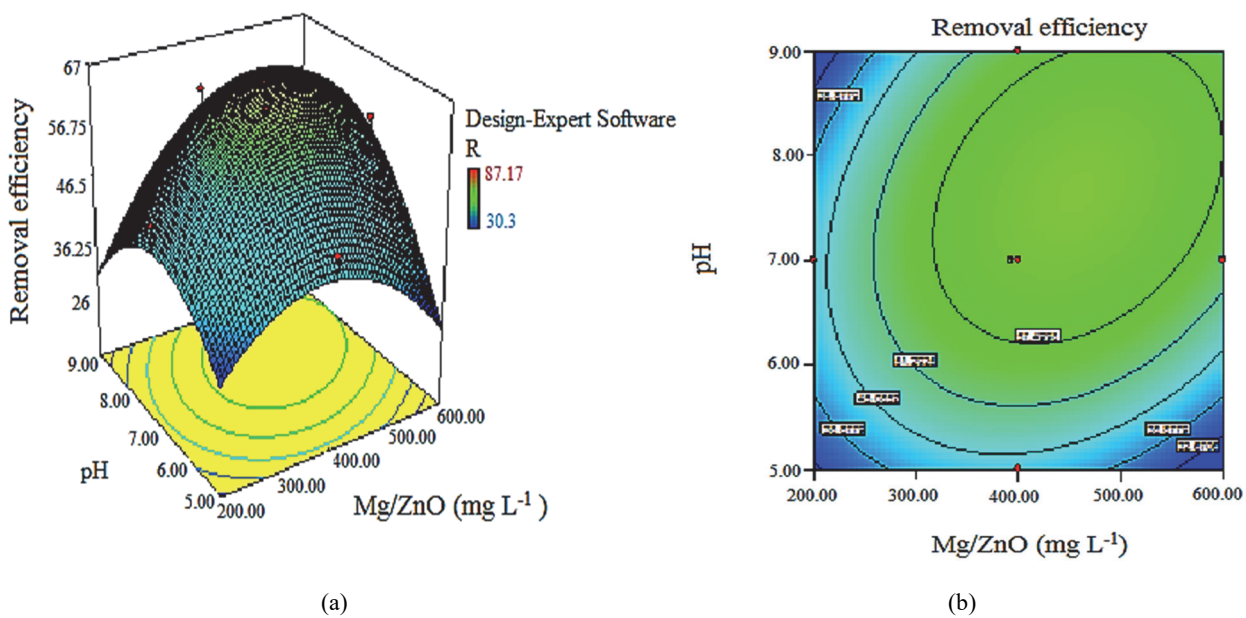


Fig. 10. (a) Response surface and (b) contour plots for photocatalytic removal efficiency of RhB (%) as a function of Mg/ZnO dosage and pH

3.4. Comparison of photocatalytic activity for Mg/ZnO nanoparticles with similar photocatalysts in the removal of RhB

In order to get more information about Mg/ZnO photocatalytic efficiency, its activity was compared with similar photocatalysts reported in the literature. Table 6 shows the removal efficiency of RhB with different photocatalysts. As seen, Mg/ZnO nanoparticles show the highest activity. One reason for this could be the appropriate synthesis method (sol-gel) used in the study. Another contributory factor may be the light source.

Although all of the studies have been carried out in the presence of UV light, there are differences among them which could affect the photocatalytic activity. The results obtained from the current study indicate that by using the sol-gel method, Mg/ZnO nanoparticles showed higher efficiency in the removal of refractory contaminant under UV-C light.

4. Conclusions

Mg 2%/ZnO nanoparticles are synthesized by the sol-gel method and used in the photocatalytic removal of RhB under UV light irradiation. In this study, the CCD was employed to optimize the removal efficiency of RhB. The dosage of Mg 2%/ZnO nanoparticles, initial RhB concentration, irradiation time and pH have the most significant effects on the removal of RhB. ANOVA results showed a correlation coefficient of 0.9354, implying that the predicted values matched the experimental values.

The optimum values when the 87.17% RhB removal is achieved were 500 mg L⁻¹ of Mg 2%/ZnO nanoparticles dosage, 6 mg L⁻¹ of initial RhB concentration, 6 min of irradiation time and pH = 8. Analysis of variance showed the accuracy of the model with high correlation coefficient (0.9354) and high F-value of 15.51. A comparison made between Mg 2%/ZnO photocatalytic activity with similar photocatalysts reported in the literature showed that the synthesized nanoparticles by sol-gel method had the highest photocatalytic removal efficiency in the

removal of RhB.

Acknowledgements

The authors are thankful to Mr. Hossein Rezaiyan Bazzaz (Assistant Researcher of Nanoparticles and Coatings Laboratory of Physics Department in the Sharif University of Technology) for kindly providing the distribution of light intensity of the lamp. The authors would like to thank the financial support of Tabriz Branch, Islamic Azad University.

References

- Ahmed S., Rasul M.G., Brown R., Hashib M.A., (2011a), Influence of parameters on the heterogeneous photocatalytic degradation of pesticides and phenolic contaminants in wastewater: A short review, *Journal of Environmental Management*, **92**, 311-330.
- Ahmed S., Rasul M.G., Martens W.N., Brown R., Hashib M.A., (2011b), Advances in heterogeneous photocatalytic degradation of phenols and dyes in wastewater: A review, *Water, Air, & Soil Pollution*, **215**, 3-29.
- Behnajady M.A., Modirshahla N., Mirzamohammady M., Vahid B., Behnajady B., (2008a), Increasing photoactivity of titanium dioxide immobilized on glass plate with optimization of heat attachment method parameters, *Journal of Hazardous Materials*, **160**, 508-513.
- Behnajady M.A., Modirshahla N., Shokri M., Rad B., (2008b), Enhancement of photocatalytic activity of TiO₂ nanoparticles by silver doping: Photodeposition versus liquid impregnation methods, *Global Nest Journal*, **10**, 1-7.
- Behnajady M.A., Ghorbanzadeh Moghaddam S., Modirshahla N., Shokri M., (2009), Investigation of the effect of heat attachment method parameters at photocatalytic activity of immobilized ZnO nanoparticles on glass plate, *Desalination*, **249**, 1371-1376.
- Behnajady M.A., Alizade B., Modirshahla N., (2011a), Synthesis of Mg-doped TiO₂ nanoparticles under different conditions and its photocatalytic activity, *Photochemistry and Photobiology*, **87**, 1308-1314.
- Behnajady M.A., Eskandarloo H., Modirshahla N., Shokri M., (2011b), Investigation of the effect of sol-gel synthesis variables on structural and photocatalytic properties of TiO₂ nanoparticles, *Desalination*, **278**, 10-17.

Table 5. Optimum values of RhB removal efficiency (%)

Mg/ZnO dosage (mg L ⁻¹)	Initial RhB concentration (mg L ⁻¹)	Irradiation time (min)	pH	Experimental removal efficiency (%)	Predicted removal efficiency (%)
500	6	6	8	87.17	83.25

Table 6. Comparison of different photocatalysts in removal of RhB

Photocatalyst	Initial concentration of RhB (mg L ⁻¹)	Photocatalyst dosage (mg L ⁻¹)	Irradiation time (min)	Removal percent	Reference
Ag/ZnO	10	400	30	85	Tian et al. (2011)
ZnO	10	400	30	57	Tian et al. (2011)
ZnO/CeO ₂	25	650	30	25	Li et al. (2012)
Ag/ZnO	5	2000	30	95	Chai et al. (2014)
ZnO	2.5	300	30	55	Giraldi et al. (2012)
Mg/ZnO	6	500	6	82.3	Present study

- Behnajady M.A., Eskandarloo H., (2013), Silver and copper co-impregnated onto TiO₂-P25 nanoparticles and its photocatalytic activity, *Chemical Engineering Journal*, **228**, 1207-1213.
- Bradley N., (2007), *The Response Surface Methodology*, MSc Thesis, Department of Mathematical Sciences, Indiana University South Bend, India.
- Chai B., Wang X., Cheng S., Zhou H., Zhang F., (2014), One-pot triethanolamine-assisted hydrothermal synthesis of Ag/ZnO heterostructure microspheres with enhanced photocatalytic activity, *Ceramics International*, **40**, 429-435.
- Chong M.N., Jin B., Chow C.W.K., Saint C., (2010), Recent developments in photocatalytic water treatment technology: A review, *Water Research*, **44**, 2997-3027.
- Cotto-Maldonado M.C., Campo T., Elizalde E., Gomez-Martinez A., Morant C., Marquez F., (2013), Photocatalytic degradation of Rhodamine-B under UV-Visible light irradiation using different nanostructured catalysts, *American Chemical Science Journal*, **3**, 178-202.
- Cun W., Jincai Z., Xinming W., Bixian M., Guoying S., Pingan P., Jiamo F., (2002), Preparation, characterization and photocatalytic activity of nanosized ZnO/SnO₂ coupled photocatalysis, *Applied Catalysis B: Environmental*, **39**, 269-279.
- Eskandarloo H., Badie A., Behnajady M.A., (2014), TiO₂/CeO₂ hybrid photocatalyst with enhanced photocatalytic activity: Optimization of synthesis variables, *Industrial & Engineering Chemistry Research*, **53**, 7847-7855.
- Eskandarloo H., Badie A., Behnajady M.A., (2015), Application of response surface methodology for optimization of operational variables in photodegradation of phenazopyridine drug using TiO₂/CeO₂ hybrid nanoparticles, *Desalination and Water Treatment*, **54**, 3300-3310.
- Esfahani A.R., Firouzi A.F., Sayyad G., Kiasat A., Alidokht L., Khataee A.R., (2014), Pb (II) removal from aqueous solution by polyacrylic acid stabilized zero-valent iron nanoparticles: Process optimization using response surface methodology, *Research on Chemical Intermediates*, **40**, 431-445.
- Fakhri A., (2015), Investigation of mercury (II) adsorption from aqueous solution onto copper oxide nanoparticles: Optimization using response surface methodology, *Process Safety and Environmental Protection*, **93**, 1-8.
- Fakhri A., Behrouz S., (2015), Comparison studies of adsorption properties of MgO nanoparticles and ZnO-MgO nanocomposites for linezolid antibiotic removal from aqueous solution using response surface methodology, *Process Safety and Environmental Protection*, **94**, 37-43.
- Georgekutty R., Seery M.K., Pillai S.C., (2008), A highly efficient Ag-ZnO photocatalyst: Synthesis, properties, and mechanism, *Journal of Physical Chemistry C*, **112**, 13563-13570.
- Giraldi T.R., Santos G.V.F., Mendonca V.R., Ribeiro C., Weber I.T., (2012), Effect of synthesis parameters on the structural characteristics and photocatalytic activity of ZnO, *Materials Chemistry and Physics*, **136**, 505-511.
- Greenwood N.N., Earnshaw A., (1997), *Chemistry of the Elements*, 2nd Edition, Butterworth-Heinemann Press, Leeds, U.K.
- Guerra W.N.A., Santos J.M.T., Araujo L.R.R., (2012), Decolorization and mineralization of reactive dyes by a photocatalytic process using ZnO and UV radiation, *Water Science & Technology*, **66**, 158-164.
- Huang K., Tang Z., Zhang L., Yu J., Lv J., Liu X., Liu F., (2012), Preparation and characterization of Mg-doped ZnO thin films by sol-gel method, *Applied Surface Science*, **258**, 3710-3713.
- Jonidi Jafari A., Dehghanifard E., Rezaei Kalantary R., Gholami M., Esrafili A., Yari A.R., Baneshi M.M., (2016), Photocatalytic degradation of aniline in aqueous solution using ZnO nanoparticles, *Environmental Engineering and Management Journal*, **15**, 53-63.
- Karthikeyan B., Pandiyarajan T., (2010), Simple room temperature synthesis and optical studies on Mg doped ZnO nanostructures, *Journal of Luminescence*, **130**, 2317-2321.
- Khalik W.F., Ong S.-A., Ho L.-N., Wong Y.-S., Yusoff N.A., Ridwan F., (2018), Comparison on solar photocatalytic degradation of orange G and new coccine using zinc oxide as catalyst, *Environmental Engineering and Management Journal*, **17**, 391-398.
- Khataee A.R., (2009), Application of central composite design for the optimization of photodestruction of a textile dye using UV/S₂O₈²⁻ process, *Polish Journal of Chemical Technology*, **11**, 38-45.
- Khataee A.R., (2010), Optimization of UV-promoted peroxydisulphate oxidation of C.I. Basic Blue 3 using response surface methodology, *Environmental Technology*, **31**, 73-86.
- Khataee A.R., Kasiri M.B., Alidokht L., (2011), Application of response surface methodology in the optimization of photocatalytic removal of environmental pollutants using nanocatalysts, *Environmental Technology*, **32**, 1669-1684.
- Khuri A.I., Mukhopadhyay S., (2010), Response surface methodology, *WIREs Computational Statistics*, **2**, 128-149.
- Li C., Zhang X., Dong W., Liu Y., (2012), High photocatalytic activity material based on high-porosity ZnO/CeO₂ nanofibers, *Materials Letters*, **80**, 145-147.
- Lin C.W., Cheng T.Y., Chang L., Juang J.Y., (2004), Chemical vapor deposition of zinc oxide thin films on Y₂O₃/Si substrates, *Physica Status Solidi (c)*, **1**, 851-855.
- Lutic D., Coromelci C.G., Juzsakova T., Cretescu I., (2017), New mesoporous titanium oxide-based photoactive materials for the removal of dyes from wastewaters, *Environmental Engineering and Management Journal*, **16**, 801-807.
- Montazerozohori M., Hoseinpour S.A., (2017), Decolorization of p-dimethylaminobenzal-rhodanine under photocatalytic process by use of titanium dioxide nanoparticles at various buffer pHs, *Environmental Engineering and Management Journal*, **16**, 1853-1858.
- Moussavi G., Borghee M., Farzadkia M., Asl R.A., (2015), Decolorization and mineralization of reactive red 198 in saline water: Performance comparison of photolysis, UV/TiO₂, and UV/ZnO processes, *Environmental Engineering and Management Journal*, **14**, 1027-1036.
- Narayana Saibaba K.V., King P., Gopinadh R., Sreelakshmi V., (2011), Response surface optimization of dye removal by using waste prawn shells, *International Journal of Chemical Sciences and Applications*, **2**, 186-193.
- Nishio J., Tokumura M., Zhand H.T., Kawase Y., (2006), Photocatalytic decolorization of azo-dye with zinc oxide powder in an external UV light irradiation slurry

- photoreactor, *Journal of Hazardous Materials*, **138**, 106-115.
- Olmez T., (2009), The optimization of Cr(VI) reduction and removal by electrocoagulation using response surface methodology, *Journal of Hazardous Materials*, **162**, 1371-1378.
- Pajootan E., Arami M., Rahimdokht M., (2014), Discoloration of wastewater in a continuous electro-Fenton process using modified graphite electrode with multi-walled carbon nanotubes/surfactant, *Separation and Purification Technology*, **130**, 34-44.
- Pi K.-W., Xiao Q., Zhang H.Q., Xia M., Gerson A.R., (2014), Decolorization of synthetic Methyl Orange wastewater by electrocoagulation with periodic reversal of electrodes and optimization by RSM, *Process Safety and Environmental Protection*, **92**, 796-806.
- Saravanathamizhan R., Mohan N., Balasubramanian N., Ramamurthy V., Ahmed Basha C., (2007), Evaluation of electro-oxidation of textile effluent using response surface methods, *Clean-Soil, Air, Water*, **35**, 355-361.
- Shaykhi Z.M., Zinatizadeh A.A.L., (2014), Statistical modeling of photocatalytic degradation of synthetic amoxicillin wastewater (SAW) in an immobilized TiO₂ photocatalytic reactor using response surface methodology (RSM), *Journal of the Taiwan Institute of Chemical Engineers*, **45**, 1717-1726.
- Sohrabi M.R., Moghri M., Fard Masoumi H.R., Amiri S., Moosavi N., (2016), Optimization of Reactive Blue 21 removal by Nanoscale Zero-Valent Iron using response surface methodology, *Arabian Journal of Chemistry*, **9**, 518-525.
- Sudamalla P., Saravanan P., Matheswaran M., (2012), Optimization of operating parameters using response surface methodology for adsorption of crystal violet by activated carbon prepared from mango kernel, *Sustainable Environment Research*, **22**, 1-7.
- Suwanboon S., Amornpitoksuk P., (2012), Preparation of Mg-doped ZnO nanoparticles by mechanical milling and their optical properties, *Procedia Engineering*, **32**, 821-826.
- Talebian N., Nilforoushan M.R., (2010), Comparative study of the structural, optical and photocatalytic properties of semiconductor metal oxides toward degradation of Methylene blue, *Thin Solid Films*, **518**, 2210-2215.
- Tian C., Zhang Q., Jiang B., Tian G., Fu H., (2011), Glucose-mediated solution-solid route for easy synthesis of Ag/ZnO particles with superior photocatalytic activity and photostability, *Journal of Alloys and Compounds*, **509**, 6935-6941.
- Trinh T.K., Kang L.S., (2010), Application of response surface method as an experimental design to optimize coagulation tests, *Environmental Engineering Research*, **15**, 063-070.
- Tzikalos N., Belessi V., Lambropoulou D., (2013), Photocatalytic degradation of reactive red 195 using anatase/brookite TiO₂ mesoporous nanoparticles: optimization using response surface methodology (RSM) and kinetics studies, *Environmental Science and Pollution Research International*, **20**, 2305-2320.
- Umar K., Haque M.M., Muneer M., Harada T., Matsumura M., (2013), Mo, Mn and La doped TiO₂: Synthesis, characterization and photocatalytic activity for the decolorization of three different chromophoric dyes, *Journal of Alloys and Compounds*, **578**, 431-438.
- Vaez M., Zarringhalam Moghaddam A., Alijani S., (2012), Optimization and modeling of photocatalytic degradation of azo dye using a response surface methodology (RSM) based on the central composite design with immobilized titania nanoparticles, *Industrial & Engineering Chemistry Research*, **51**, 4199-4207.
- Viswanatha R., Arthoba Nayaka Y., Vidyasagar C.C., Venkatesh T.G., (2012), Structural and optical properties of Mg doped ZnO nanoparticles, *Journal of Chemical and Pharmaceutical Research*, **4**, 1983-1989.
- Wu C.H., Chang C.L., (2006), Decolorization of reactive red 2 by advanced oxidation processes: comparative studies of homogeneous and heterogeneous systems, *Journal of Hazardous Materials*, **128**, 265-272.
- Xianyong L., Zhaoyue L., Ying Z., Lei J., (2011), Sonochemical synthesis and photocatalytic property of zinc oxide nanoparticles doped with magnesium(II), *Materials Research Bulletin*, **46**, 1638-1641.
- Xu H.Y., Qi S.Y., Li Y., Zhao Y., Li J.W., (2013), Heterogeneous fenton-like discoloration of Rhodamine B using natural schorl as catalyst: optimization by response surface methodology, *Environmental Science and Pollution Research*, **20**, 5764-5772.
- Zarei N., Behnajady M.A., (2016), Synthesis, characterization, and photocatalytic activity of sol-gel prepared Mg/ZnO nanoparticles, *Desalination and Water Treatment*, **57**, 16855-16861.
- Zhao S., Huang G., Cheng G., Wang Y., Fu H., (2014), Hardness, COD and turbidity removals from produced water by electrocoagulation pretreatment prior to Reverse Osmosis membranes, *Desalination*, **344**, 454-462.
- Zolgharnein J., Asanjarani N., Mousavi S.N., (2010), Optimization and characterization of Tl(I) adsorption onto modified ulmus carpinifolia tree leaves, *Clean – Soil, Air, Water*, **39**, 250-258.
- Zuorro A., Fidaleo M., Lavecchia R., (2013), Response surface methodology (RSM) analysis of photodegradation of sulfonated diazo dye reactive green 19 by UV/H₂O₂ process, *Journal of Environmental Management*, **127**, 28-35.